Electronic Supplementary Material (ESI) for Catalysis Science & Technology.
This journal is © The Royal Society of Chemistry 2024

Supporting information

Electronic Regulation & Improved Conductivity of Molecular Catalysts as Electrocatalysts

Hu Bihua [a,b], *Cao Hailin* [c], *Lei Zhiwei* [a], *Cui Shuyu* [a], *Wang Peizhi* [a], *Tang Jun* [b,*], *Wang Xingzhu* [a,d,*], *Xu Baomin* [a,*]

[a]Department of Materials Science and Engineering, Southern University of Science and Technology, Shenzhen 518055, China
[b]College of New Materials and New Energies, Shenzhen Technology University, Shenzhen 518118, China
[c]Department of Mechanical and Energy Engineering, Southern University of Science and Technology, Shenzhen 518055, China
[d]Shenzhen Putai Technology Co., Ltd, Shenzhen, 518055, China

[†]These authors contributed equally to this work.

[*]Corresponding author

E-mail: tangjun3@sztu.edu.cn (J. Tang); wangxz@sustech.edu.cn (X. Wang); xubm@sustech.edu.cn (B. Xu)

Table of Contents

Supplementary Note 1. Materials

Titanium powder, Aluminum powder Iron phthalocyanine (FePc), Phthalocyanine cobalt (CoPc), Nickel phthalocyanine (NiPc) and Zinc phthalocyanine (ZnPc) were purchased from Shanghai Aladdin, China. Raw CNTs and N-CNTs (diameter = 30-50 nm, length = 0.5-2 μm) were purchased from Nanjing XFNANO Materials Tech Co. Ltd. Ethanol was obtained from Tianjin Chemical Reagent Co. China. N, N-Dimethylformamide (DMF), Polytetrafluoroethylene (PTFE, 60 wt.%, emulsion) and Nafion® (5 wt.%) were purchased from Shanghai Aladdin Reagent Co., Ltd. All other reagents, including $KHCO_3$, HCl, D_2O and C_2H_5OH were purchased from Guangzhou Chemical Reagent Factory. All reagents were of analytical grade and used without further purification. Deionized water was used in all experiments.

Supplementary Note 2. Experimental methods

2.1 Synthesis of catalysts

2.1.1 Synthesis of Ti_3C_2Al (MAX)

CNTs, Ti powder and Al powder were mixed in a ratio of 2:3:1, then ground in the glove box for half an hour, after which the powder was heated in a furnace for 2 h at 1400 °C in Ar atmosphere. After the furnace is cooled to room temperature, the product is taken out and soaked in concentrated hydrochloric acid for 2 h to remove the incomplete reaction powder in the product. The slurry was then diluted, centrifuged and cleaned, and afterwards dried overnight in a vacuum oven at 60 °C.

2.1.2 Synthesis of $Ti_3C_xN_{2-x}Al$ (N-MAX)

N-CNTs, Ti powder3and Al powder was first mixed in a ratio of 2:3:1 and then ground in the glove box for half an hour. The subsequent processing is the same as synthesis of MAX.

2.1.3 Synthesis of Ti_3C_2 (MXene)

Take 6 ml of H_2O, add 12 ml of HCl, 2.5 ml of HF, stir well, then add 1 g of MAX, place in an oil bath at 35 °C for 24 h. After heating, take out the slurry, wash with deionized water to pH value of neutral, then add 60 ml of deionized water to disperse, add 1 g of LiCl, placed in an oil bath at 35 °C for heating and stirring for 4 h, after washing and shaking evenly, the MXene solution was obtained.

2.1.4 Synthesis of $Ti_3C_{2-x}N_x$ (N-MXene)

The same synthesis procedure as for MXene is used to replace MAX with N-MAX.

2.1.5 Synthesis of MPc/MXene and MPc/N-MXene) (M-Fe, Co, Ni, Zn)

MPc-MXene hybrid (20 wt. MPc%) was prepared by interacting MPc and MXene in N, N-dimethyl formamide (DMF) with the assistance of magnetic stirring and sonication for 24 h. The solution is then filtered with suction, and the solid obtained after the freeze-drying is the catalyst needed. When MXene is replaced with N-MXene and the step above is repeated, we can get MPc/N-Mxene.

2.1.6 Synthesis of MPc/o-N-MXene by in-situ anodic oxidation

MPc/o-N-MXene was obtained by in-situ oxidation of MPc/N-MXene with Cyclic voltammetry scan at 10 mV s^{-1} at various potentials from -1.2 V to 2.48 V (vs RHE) for 16s in $KHCO_3$ electrolyte. To determine the optimal degree of oxidation, we performed different degrees of oxidation in a 2, 8, 16, and 50s Cyclic voltammetry (CV) scan at 10 mV s^{-1} at various potentials from -1.2 V to 2.48 V (vs RHE), and performed ERCD at -1.0 V for 30 min, then collected the liquid product (DMSO as a yardstick) combined with the corresponding current density for comparison, as shown in Fig. S14-15, as the degree of oxidation of CoPc/o-N-MXene increases, the current density decreases gradually, while the absolute yield of methanol increases gradually, considering the influence of the degree of oxidation on the current density and the methanol yield, we chose the degree of oxidation in a 16s Cyclic voltammetry scan at 10 mV s^{-1} at various potentials from -1.2 V to 2.48 V (vs RHE).

2.2 Characterization

2.2.1 Catalysts characterization

X-ray diffraction (XRD) measurements were examined with a Bruker ECO D8

diffractometer with Cu K radiation (40 kV, 25 mA) at a scan rate of 10°min^{-1} from 5 to 75°. *Scanning electron microscope* (SEM) tests were performed using a Zeiss (Merlin) scanning electron microscope at an accelerating voltage of 5 KV. *Scanning/transmission electron microscopy* (S/TEM) images were taken on an FEI Talos F200X operated at an acceleration voltage of 200 kV. Before TEM measurements, the catalysts were dispersed in an ethanol solution by an ultrasonic water bath, and then dried onto Microgrids. *X-ray photoelectron spectroscopy* (XPS) tests were conducted using a VG Scientific ESCALAB250 instrument equipped with an Al Kα X-ray source (1486.6 eV). The obtained spectrograms were analyzed employing the Xpspeak 41 software. Extended X-ray absorption fine structure (EXAFS) experiments were performed at the Taiwan Photon Source (TPS) operated at 3.0 GeV with a beam current of 500mA. The Co K-edge absorbance of the powder catalysts was measured in the transmission geometry at room temperature. The energy was scanned from -200 eV below to 600 eV above the Co K edge (7709 eV).

2.2.2 Electrochemical characterization

Electrochemical evaluations were carried out on a Chenhua electrochemical working station (CHI660E) in a conventional three-electrode electrochemical H-type cell separated by a proton exchange membrane (Nafion®-117 membrane, DuPont Company) at ambient temperature and pressure system. Ag/AgCl electrode (saturated KCl) and platinum gauze electrode (1.0 cm * 1.0 cm) were used as the reference and counter electrodes, respectively. Both cathode and anode cells were filled with an aqueous solution of 10.0 mL of 0.5 M $KHCO_3$ as the electrolyte with CO_2 continuously

bubbled into the cells at a speed of 20 mL min^{-1}. The pH value of the electrolyte saturated with CO_2 (99.99%) was 7.20.

ERCD was also performed in a three-channel flow cell composed of a gas diffusion layer (GDL), an anion exchange membrane (Fumasep, FAA-3-PK-130) and a carbon paper (1 cm^2) anode. 1.0 M KOH aqueous solution was used as anodic electrolyte, while 1.0 M $KHCO_3$ (pH = 7.5) aqueous solution was adopted as cathodic electrolyte. Both electrolytes were circulated by a two-channel peristaltic pump (NKCP-C-S10B) with a flow rate of 20 mL min^{-1}. The gas flow channel behind the GDL was constantly purged with CO_2 gas at a flow rate of 50 mL min^{-1}. To ensure that the potential trapped gas in the electrolyte was collected and thoroughly mixed with the exit gas before entering the Gas Chromatography, the electrochemical cell was entirely sealed, and a unique buffer cell was created and implemented. The potential is manually corrected for the flow cell test by subtracting the IR drop.

The working electrode was prepared as followings: a 500 μL solution of isopropanol containing 1 mg of catalyst was combined with 2 mg of carbon black (Vulcan XC-72R). Subsequently, 500 μL of deionized water and 20 μL Nafion solution (5 wt%) were added and the resulting solution was sonicated in an ice water bath for 30 min to obtain a well-dispersed catalyst slurry. Then the catalyst slurry was dropped on both sides of carbon paper (1.0 cm × 0.5 cm) for H-cell testing or on a single-sided carbon paper (2.0 cm × 0.5 cm) for flow cell testing. The area of the working electrode was 1.0 cm^2 and the catalyst loading (on a gold basis) was 1 mg cm^{-2}. Finally, the working electrode was obtained after being dried in a vacuum oven overnight.

Linear sweep voltammetry (LSV) was recorded with a scan rate of 10 mV s^{-1}. Cyclic voltammograms (CV) with a scan rate of 100 mV s^{-1} were used to clean the electrode surfaces. Controlled-potential electrolysis was performed to quantify the activity and selectivity of catalysts toward ERCD. The measurement of Faradaic efficiency (FE) was further carried out under the condition that the different electrode potentials were maintained for 30 min. It should be noted that, without specification, all the potentials reported in this work are iR corrected and converted versus RHE (reversible hydrogen electrode) according to the following expression:

$$E_{vs.\,RHE} = E_{vs.\frac{Ag}{AgCl}} + 0.197\,V + 0.0591\,pH \#(1)$$

2.2.3 Product analysis

The gas products were detected in-situ by gas chromatography (GC). Liquid products were collected after each constant potential test and then prepared into a nuclear magnetic sample (40 μl DMSO + 60 μl D_2O + 500 μl liquid products) for nuclear magnetic resonance detection (NMR).

The Faradaic efficiency of H_2 and CO is calculated from the peak area of the GC chromatogram at a given potential as follows:

$$i_{CO\ or\ H_2} = v_{CO\ or\ H_2} \times V \times \frac{2Fp_0}{RT} \#(2)$$

$$FE_{CO\ or\ H_2} = \frac{i_{CO\ or\ H_2}}{i_{total}} \times 100\% \#(3)$$

$i_{CO\ or\ H_2}$: Partial current density for CO or H_2

$v_{CO\ or\ H_2}$: Volume concentration of CO or H_2 based on the calibration of GC

V: Gas volume flow rate controlled by a mass flow meter at room temperature and

under ambient pressure

F: Faradaic constant, 96485 C mol^{-1}

p_0: Pressure, Pa

R: Ideal gas constant, 8.314 J $(mol \times K)^{-1}$

T: Temperature, K

$FE_{CO\ or\ H_2}$: Faradaic efficiency for CO or H_2, %

i_{total} : Total current density, mA cm^{-2}

The Faradaic efficiency of CH_3OH is calculated through the standard NMR curve (the 1H spectrum was measured with water suppression):

$$FE_{methanol} = \frac{6Fn_{methanol}}{Q} \times 100\% \#(4)$$

$FE_{methanol}$: Faradaic efficiency for methanol, %

F: Faradaic constant, 96485 C mol^{-1}

$n_{methanol}$: Mole of methanol, mol. Here, it should be noted that, in the case of NMR measurements for the standard curve, each methanol sample was tested 3 times.

Q (C): Total charge passing through the electrode during electrolysis.

Supplementary Note 3. Density functional theory calculations

Theoretical calculations were performed on the basis of density functional theory (DFT), as implemented in the Vienna ab initio simulation packages (VASP) [1]. For geometric optimizations, we have adopted Perdew-Burke-Ernzerhof [2] functional and projector augmented wave (PAW) scheme [3]. All atomic coordinates were allowed to relax until calculated Hellmann-Feynman forces smaller than 0.05 eV/Å in geometric optimization. The plane wave expansion was chosen and cutoff at the kinetic energy of 400 eV. The simulated unit cells are constructed periodically, where the vacuum space was specified to be 15 Å. In addition, the Brillouin zones were sampled by a (1×1×1) grid generated with Monkhorst-Pack scheme [4]. Explicit solvation model with a monolayer of water has been considered to calculate the solvation energies. By introducing a hydronium in the solvent, the charge was transferred between the water layer and electrode, resulting in a local electric field, which was employed to consider the electric field effects in experimental measurements.

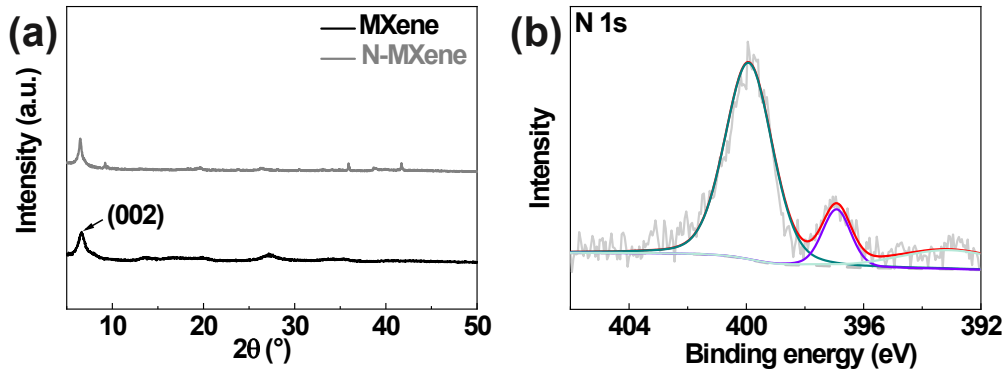

Supplementary Figure 1. Structural characterization of MXene and N-MXene. (a) XRD, (b) High-resolution N 1s XPS spectra.

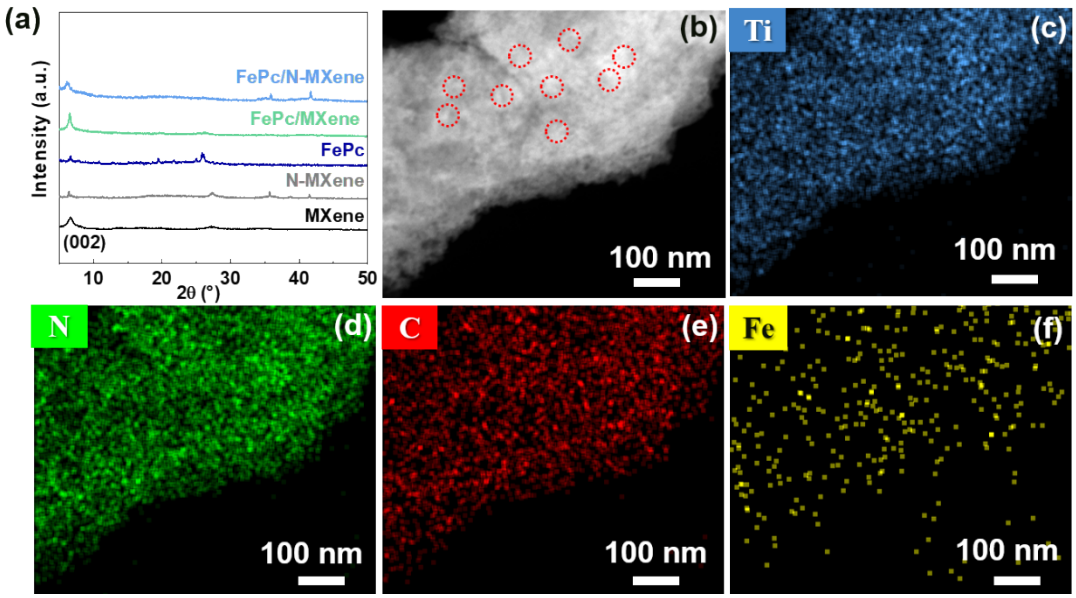

Supplementary Figure 2. Structural and morphological characterizations of the FePc, MXene FePc/MXene, and FePc/N-MXene hybrid. (a) XRD spectra; HAADF TEM of FePc/N-MXene (b) and (c-f) EDS maps of Ti (c), N (d), C (e) and Fe (f).

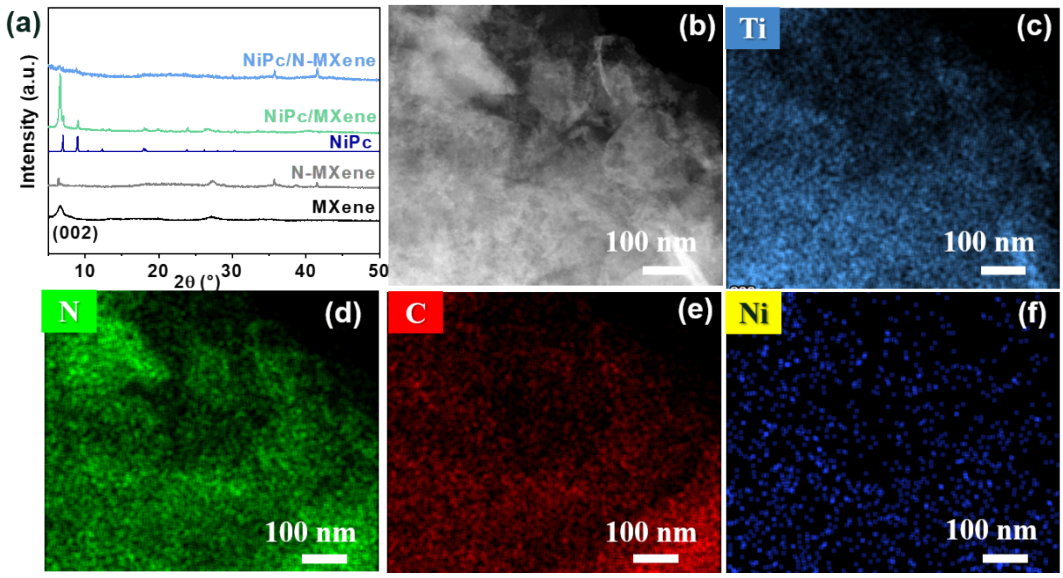

Supplementary Figure 3. Structural and morphological characterizations of the NiPc, MXene NiPc/Mxene, and NiPc/N-MXene hybrid. (a) XRD spectra; HAADF TEM of NiPc/N-MXene (b) and (c-f) EDS maps of Ti (c), N (d), C (e) and Ni (f).

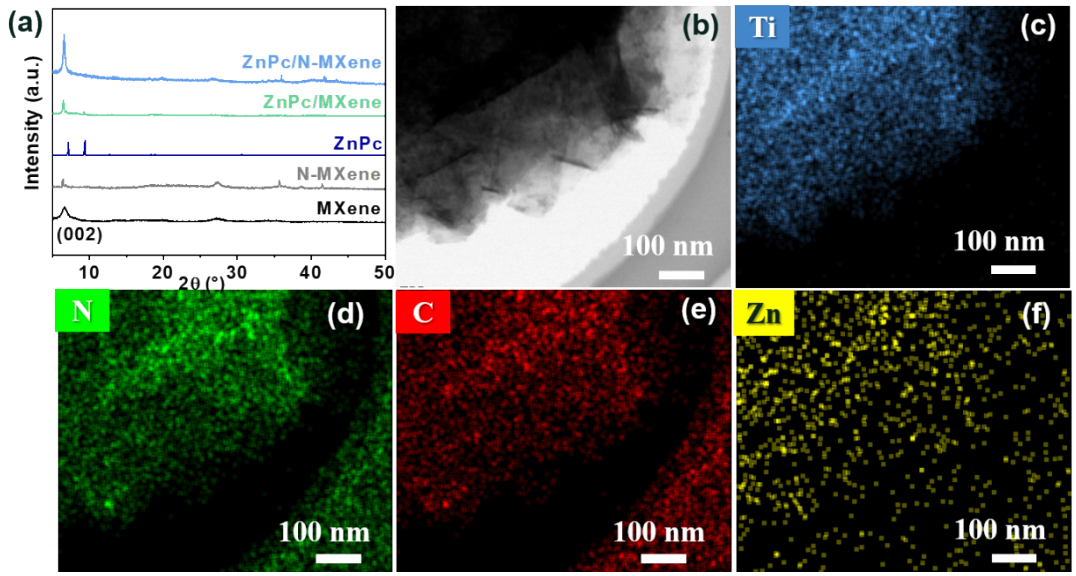

Supplementary Figure 4. Structural and morphological characterizations of the ZnPc, MXene ZnPc/Mxene, and ZnPc/N-MXene hybrid. (a) XRD spectra; HAADF TEM of ZnPc/N-MXene (b) and (c-f) EDS maps of Ti (c), N (d), C (e) and Zn (f).

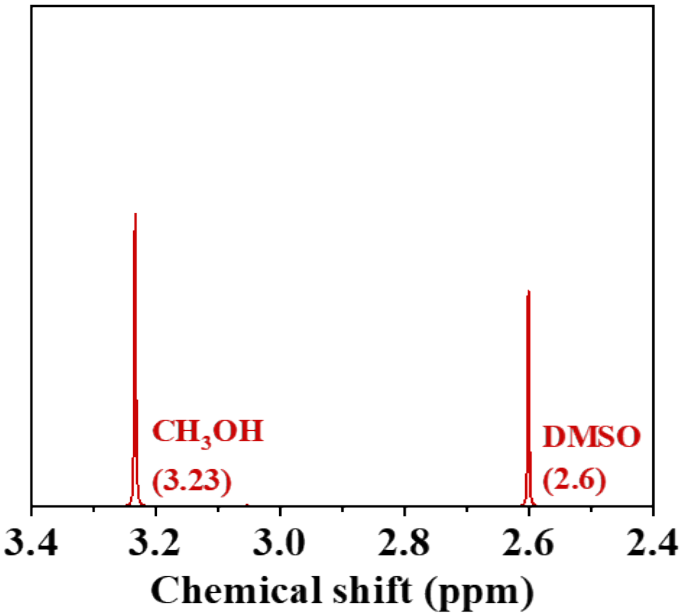

Supplementary Figure 5. NMR's standard curve of methanol.

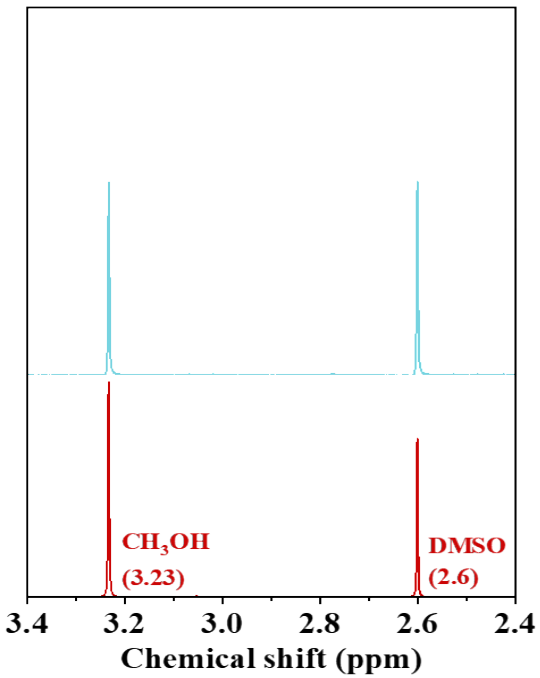

Supplementary Figure 6. NMR's curve of products, which was produced during the electrochemical reduction on CoPc/o-N-MXene electrodes in CO_2 saturated 0.5 M $KHCO_3$.

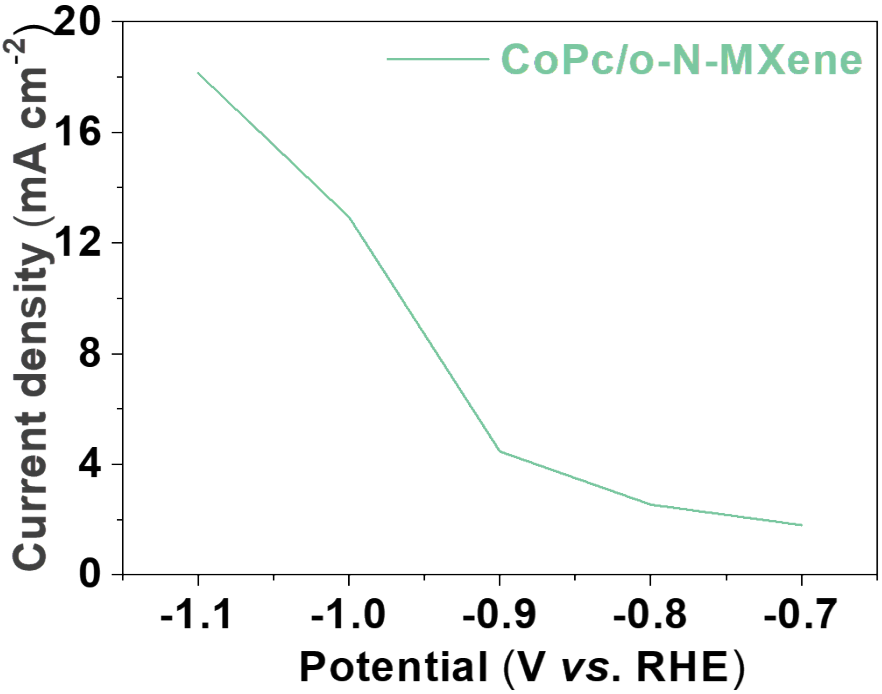

Supplementary Figure 7. The partial current density of methanol at the CoPc/o-N-MXene toward ERCD in a CO_2 saturated 0.5 M $KHCO_3$ solution at various potentials via from -0.7 V to -1.1 V (*vs.* RHE) (at an interval of -0.1 V).

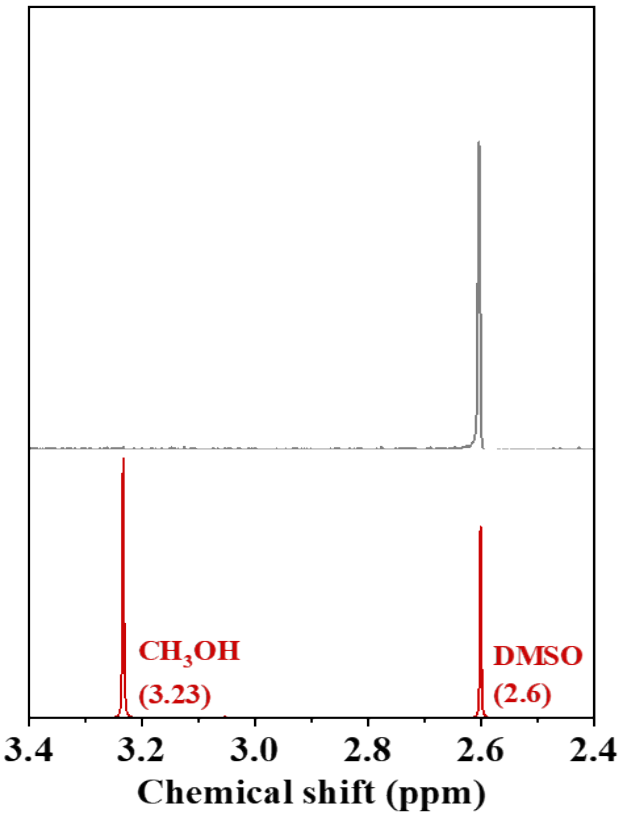

Supplementary Figure 8. NMR's curve of products, which was produced during the electrochemical reduction on CoPc/o-N-MXene electrodes in N_2 saturated 0.5 M $KHCO_3$.

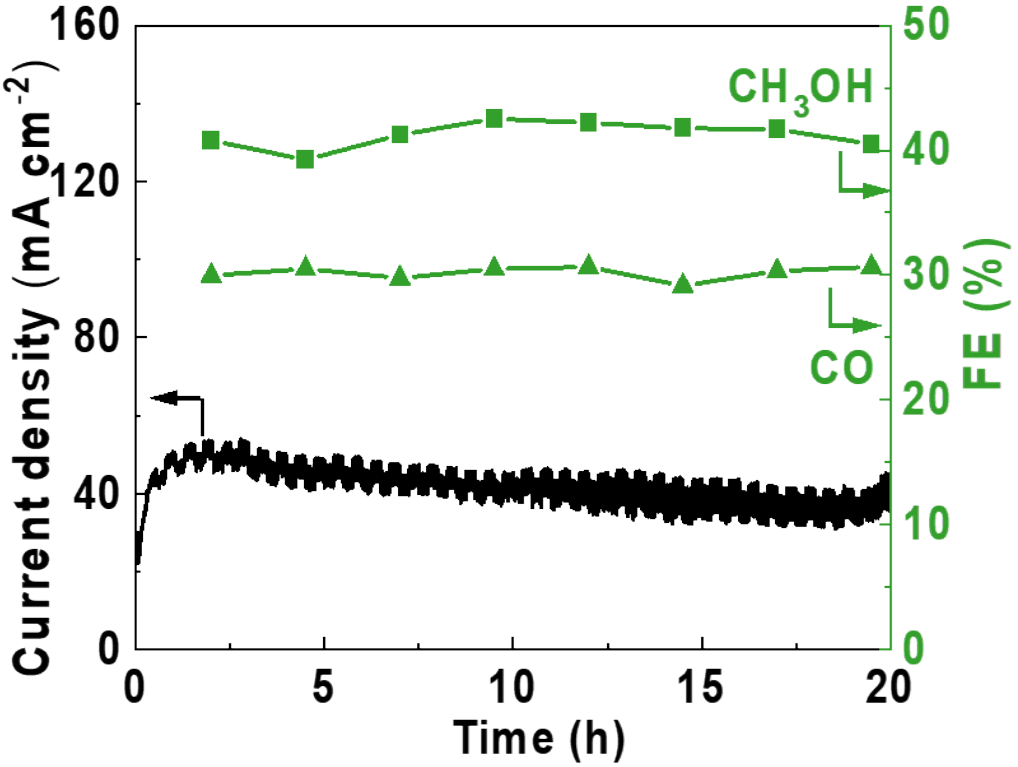

Supplementary Figure 9. Longevity test of CoPc/o-N-MXene toward ERCD in a CO_2 saturated 0.5 M $KHCO_3$ solution at -1.0 V (*vs.* RHE).

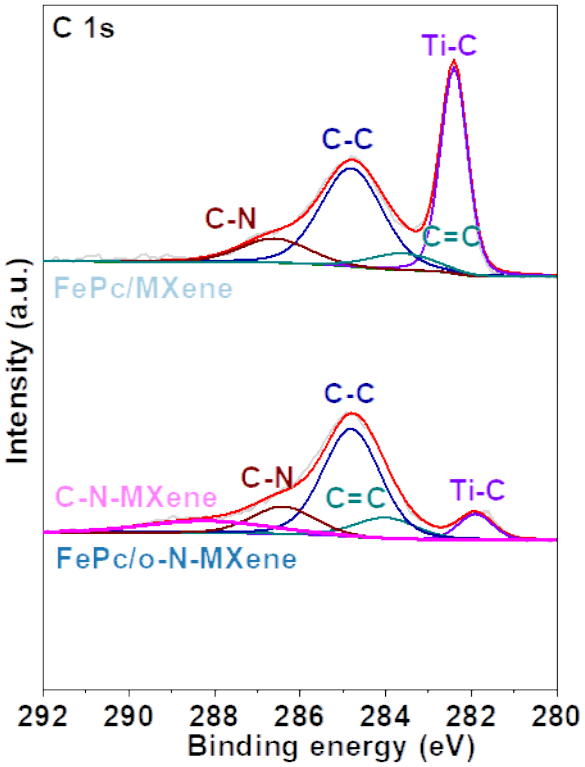

Supplementary Figure 10. High-resolutionC 1s spectra of FePc/MXene and FePc/o-N-MXene.

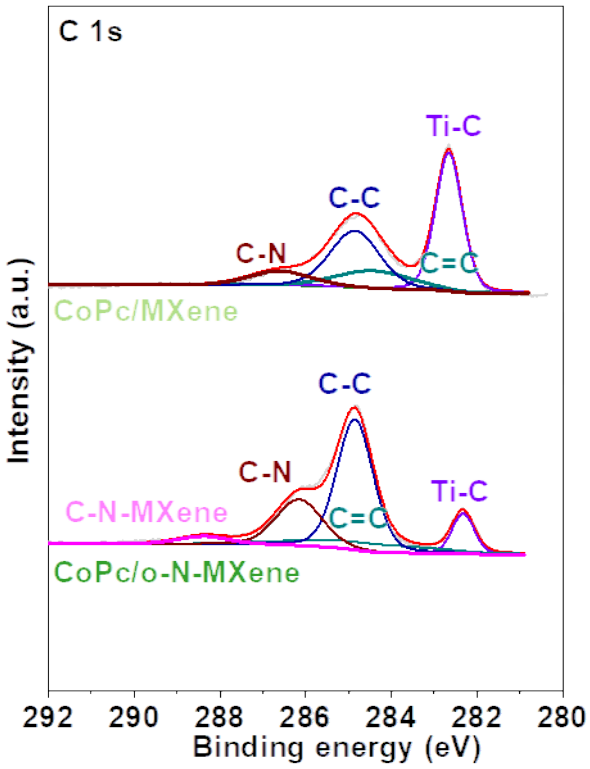

Supplementary Figure 11. High-resolutionC 1s spectra of CoPc/MXene and CoPc/o-N-MXene.

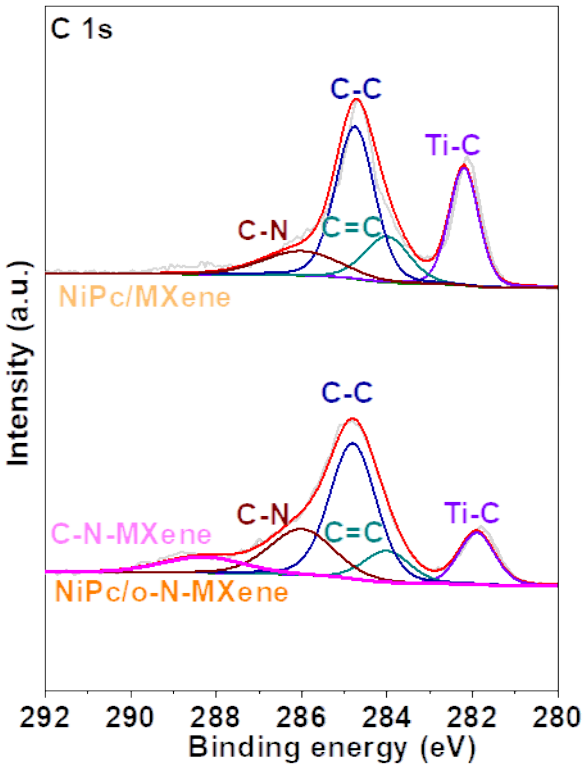

Supplementary Figure 12. High-resolutionC 1s spectra of NiPc/MXene and NiPc/o-N-MXene.

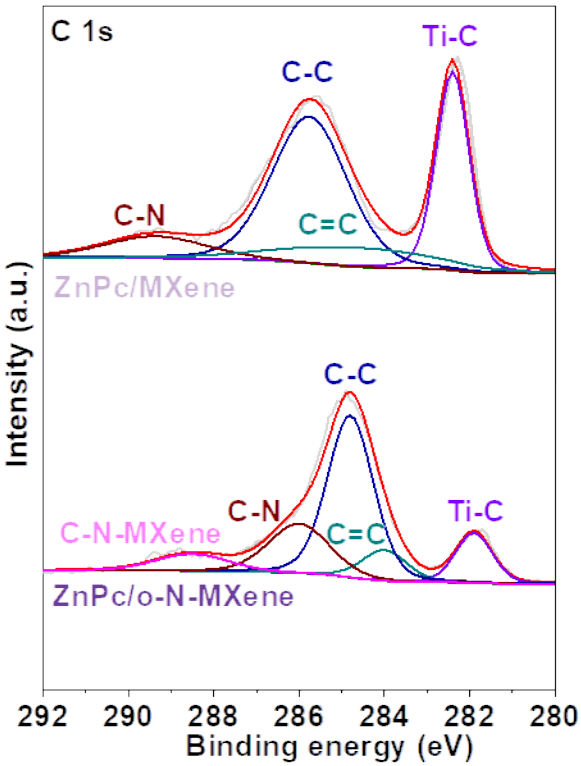

Supplementary Figure 13. High-resolutionC 1s spectra of ZnPc/MXene and ZnPc/o-N-MXene.

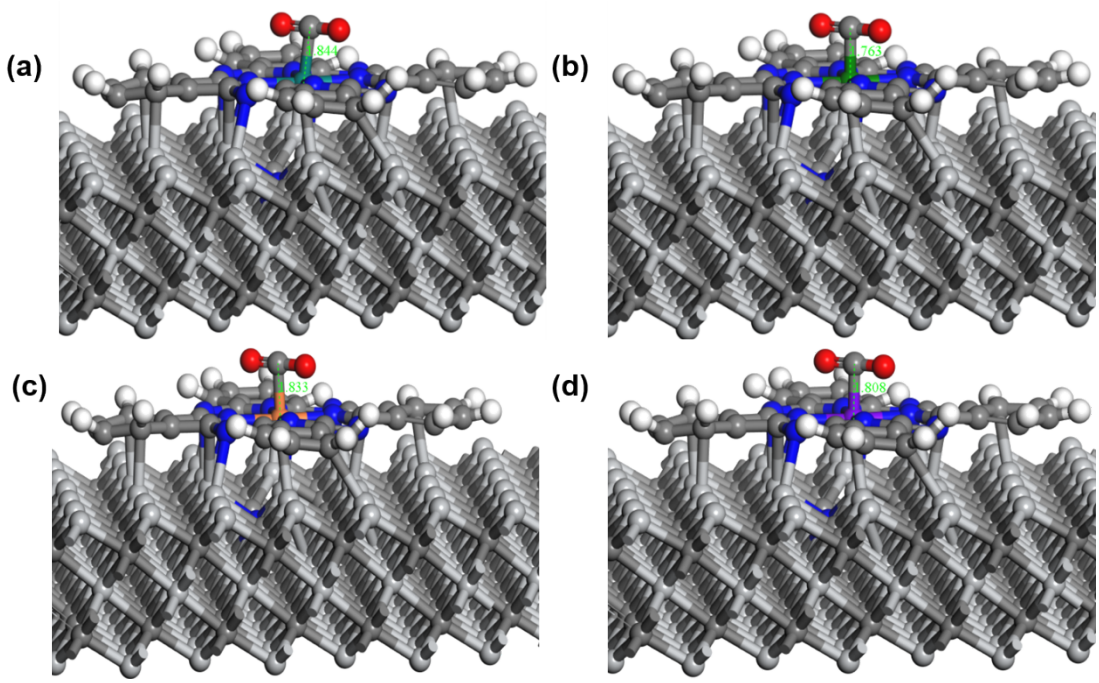

Supplementary Figure 14. The adsorption models of CO_2 adsorbed on MPc/o-N-MXene (M-Fe, Co, Ni, Zn): FePc/o-N-MXene (1.844) (a), CoPc/o-N-MXene (1.763) (b), NiPc/o-N-MXene (1.833) (c), ZnPc/o-N-MXene (1.808) (d).

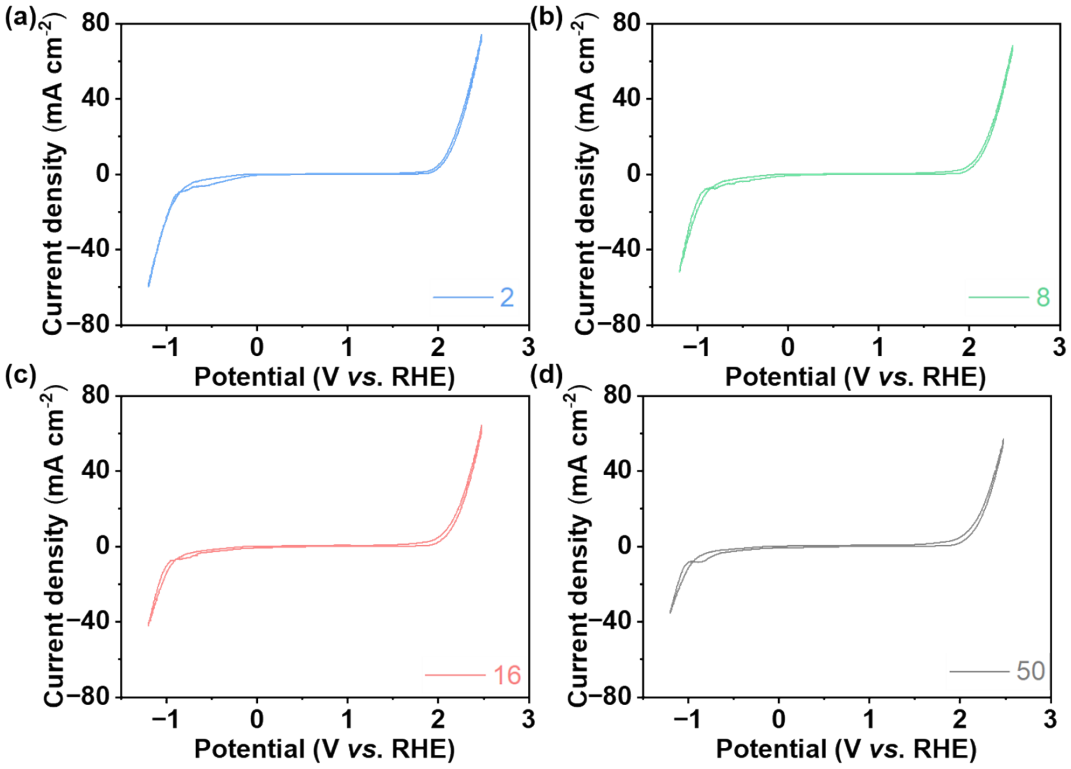

Supplementary Figure 15. Oxidation of the CoPc/N-MXene: 2 (a), 8 (b), 16 (c), 50s (d) of CV at a scan rate of 10 mv/s in CO_2 saturated 0.5 M $KHCO_3$ solution via potential from -1.2 V to 2.48 V (vs. RHE).

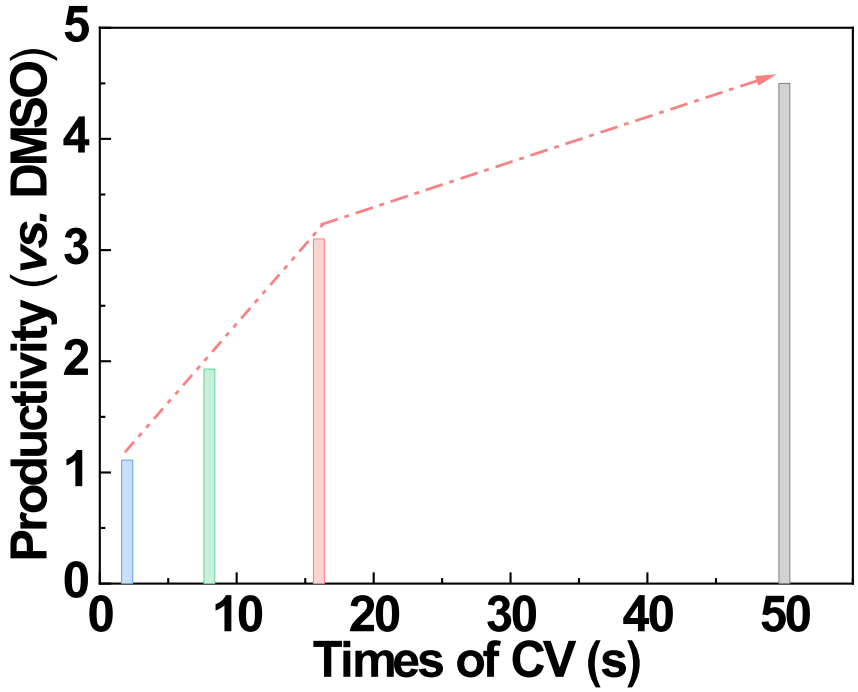

Supplementary Figure 16. Methanol produced by potentiostatic test at -1.2 V (*vs*. RHE) after 2, 8, 16, 50s of CV at a scan rate of 10 mv/s in CO_2 saturated 0.5 M $KHCO_3$ solution via potential from -1.2 V to 2.48 V (vs. RHE).

Supplementary Table 1. Quantitative analysis of N-MXene.

Name	Area (P) CPS.eV	Area (N)	Atomic %
C1s	40849.35	0.93	60.92
N1s	6059.13	0.08	5.55
Ti2p	139220.7	0.51	33.54

Supplementary Table 2. Bader charge for M of MPc/o-N-MXene (M-Fe, Co, Ni, Zn) before and after HCO adsorbed.

Name	Bader charge before HCO adsorbed (|e|)	Bader charge after HCO adsorbed (|e|)
Fe	2.3998	2.3766
Co	2.3954	2.7860
Ni	2.3028	2.3017
Zn	2.3615	2.3214

Supplementary References

[1] H. Yang, C. Sun, S. Qiao, J. Zou, G. Liu, S. Smith, H. Chen, G. Lu, *Nature*, **2008**, 453, 638-641.

[2] J. Perdew, K. Burke, M. Ernzerhof, *Phys. Rev. Lett.,* **1996**, 77, 3865-3868.

[3] L. Schimka, J. Harl, A. Stroppa, M.Marsman, F. Mittendorfer, G. Kresse, *Nat. Mater.,* **2010**, 9, 741-744.

[4] H. Monkhorst, J. Pack, *Phys. Rev. B,* **1976**, 13, 5188-5192.